Hydration of the Fluoride Anion: Structures and Absolute Hydration Free Energy from First-Principles Electronic Structure Calculations

Chang-Guo Zhan*,† and David A. Dixon*,‡

Fundamental Sciences Directorate, Pacific Northwest National Laboratory, MS K9-90, P.O. Box 999, Richland, Washington 99352

Received: October 9, 2003; In Final Form: November 26, 2003

A series of first-principles electronic structure calculations have been performed to determine the most stable structures of $F^-(H_2O)_n$ clusters ($n = 4$, 8, 12, and 16) and the hydration free energy of fluoride anion (F^-). The calculated results show that a new, tetrahedrally coordinated fluoride anion hydration structure $F^-(H_2O)_4$ cluster is lower in Gibbs free energy than the previously considered most stable structure of $F^-(H_2O)_4$. The first ab initio prediction of potential stable hydration structures for $F^-(H_2O)_n$ clusters ($n = 8$, 12, and 16) are given. The energetic results show that the tetrahedrally coordinated fluoride anion hydration structure becomes more stable as compared to the other hydration structures with a pyramidal coordination, i.e., a surface ion cluster state, as the cluster size increases from $n = 8$ to $n = 12$ to $n = 16$. This suggests that, with increasing n, the fluoride anion will be internally solvated in large enough $F^-(H_2O)_n$ clusters. These results provide insight into the transition from the hydration structure found in small gas-phase hydrated-anion clusters to the hydration structure observed in aqueous solution. The calculated results show that, for a given n, the bulk solvent effects can qualitatively change the relative thermodynamic stability of different possible isomers of $F^-(H_2O)_n$ clusters and the most stable structure in solution is not necessarily the most stable structure in the gas phase. When $n = 16$, a pyramidally coordinated fluoride anion hydration structure is the most stable structure in the gas phase, whereas a tetrahedrally coordinated fluoride anion hydration structure has the lowest free energy in solution. The absolute hydration free energy of fluoride anion in aqueous solution, $\Delta G_{hyd}^{298}(F^-)$, is predicted to be -104.3 ± 0.7 kcal/mol by using a reliable computational protocol of first-principles solvation-included electronic structure calculations. The predicted $\Delta G_{hyd}^{298}(F^-)$ value of -104.3 ± 0.7 kcal/mol, together with our previously calculated $\Delta G_{hyd}^{298}(H^+)$ value of -262.4 kcal/mol determined by using the same computational protocol, gives $\Delta G_{hyd}^{298}(F^-) + \Delta G_{hyd}^{298}(H^+) = -366.7 \pm 0.7$ kcal/mol in excellent agreement with the value of -366.5 kcal/mol derived from the available experimental data.

Introduction

The hydration of ions plays an important role in aqueous chemical and biological systems.[1−11] Hydration of the fluoride anion (F^-) has been the subject of both computational and experimental studies. Recent computational and experimental studies of F^- hydration include the following: structural studies, molecular dynamics simulations, studies of the vibrational spectra, ultraviolet (UV) absorption spectral measurements, photoelectron spectral measurements, binding energy determinations, and determinations and predictions of the hydration free energy.[11−23] Despite these extensive studies, many fundamental structural, spectroscopic, and energetic questions still remain unanswered. For example, most of the ab initio computational studies have been focused on the structures and spectra of small $F^-(H_2O)_n$ clusters ($n \leq 6$) in the gas phase. A recently reported vibrational spectroscopic study[11] suggests that even the structure of the $F^-(H_2O)_4$ cluster is not completely understood. The reported vibrational spectrum[11] of the $F^-(H_2O)_4$ cluster shows that the F^- anion is coordinated by four equivalent water molecules in the $F^-(H_2O)_4$ cluster in terms of having a "free O−H bond" without hydrogen bonding, whereas the previous ab initio computational studies suggested a nonequivalent coordination[14] in the lowest energy cluster structure. This suggests that the geometry of the most stable cluster structure is not well-established.

Our recent ab initio molecular orbital theory and density functional theory studies on the chemical structure of the hydrated electron[24] show that bulk solvent effects can qualitatively change the relative thermodynamic stability of different structures of the hydrated electron based on a cluster of a given size and that the most stable structure in solution is not necessarily the most stable one in the gas phase. Whether this is also true for $F^-(H_2O)_n$ structures still needs to be addressed.

The value of the absolute solvation free energy of an ion in water, e.g., $\Delta G_{hyd}^{298}(F^-)$, is an important quantity in understanding the equilibrium thermodynamic properties and chemical reactions of a solvated ion. However, the exact value of this quantity for a given ion often has large error bars for many ions because the absolute solvation free energy of a charged species is inherently difficult to measure. Any stable, macroscopic solution contains equal amounts of positive and negative charge,[1,2] so without using additional approximations or models, an experiment can only be performed to determine the sum of solvation free energies of a pair of oppositely charged species. It has not yet been possible to isolate one type of charged species and measure its absolute solvation free energy. Thus, direct experimental data for different pairs of charged species can

† Permanent address: Division of Pharmaceutical Sciences, College of Pharmacy, University of Kentucky, 907 Rose St., Room 501B, Lexington, KY 40536. E-mail: zhan@uky.edu.

‡ Permanent address: Department of Chemistry, The University of Alabama, Tuscaloosa, AL. E-mail: dadixon@bama.ua.edu.

10.1021/jp0311512 CCC: $27.50
Published on Web 02/25/2004

provide information only about the relative magnitudes of the ionic solvation free energies.[25−27] This usually leads to ranges of values for the "experimental" absolute hydration free energy of ions, and for example, $\Delta G_{hyd}^{298}(F^-)$, has a range from −102 to −112 kcal/mol.[28] Similarly, the reported "experimental" absolute hydration free energy of the proton, $\Delta G_{hyd}^{298}(H^+)$, ranges from −252.6 to −264.1 kcal/mol,[29] and that of hydroxide ion, $\Delta G_{hyd}^{298}(HO^-)$, ranges from −90.6 [30] to −110.0 kcal/mol.[31] Reliable first-principles theoretical approaches are highly desired to predict the hydration structure and absolute hydration free energy of F^- in water. Previous electronic structure calculations reported by Topol et al.[28] predicted a theoretical $\Delta G_{hyd}^{298}(F^-)$ value of ∼ 99.86 kcal/mol. This theoretical value is close to the lower limit of the above experimental range, but it is based on a simpler solvation model as well as relatively modest levels of electronic structure theory.

We have developed a hybrid supermolecule-continuum approach[32−34] in which part of the solvent surrounding the solute is treated quantum mechanically at a high level and the remaining bulk solvent is approximated by a dielectric continuum medium model. We employ a recently developed self-consistent reaction field model known as the surface and volume polarization for electrostatic interaction (SVPE)[35] or the fully polarizable continuum model (FPCM).[36] With this approach, the calculated results can systematically be improved and converged by increasing the number of explicit solvent molecules included in the quantum chemical calculation. This approach has been employed to predict activation energies for ion−molecule reactions[32] and absolute hydration free energies of ions[33,34] and the hydrated electron[24] with high accuracy. For example, the $\Delta G_{hyd}^{298}(H^+)$, $\Delta G_{hyd}^{298}(Li^+)$, $\Delta G_{hyd}^{298}(HO^-)$, and $\Delta G_{hyd}^{298}(e^-)$ values have accurately been predicted to be −262.4, −125.1, −104.5, and −35.5 kcal/mol, respectively.[33,34] The calculated difference of 137.3 kcal/mol between the absolute hydration free energies of the proton and Li^+ is in excellent agreement with the experimental differences of 137.5 kcal/mol from the latest collection of experimental data[26] and of 137.0 kcal/mol from earlier experimental data.[30] The calculations allow us to predict the sum of absolute hydration free energies of the proton and hydroxide ion, $\Delta G_{hyd}^{298}(HO^-) + \Delta G_{hyd}^{298}(H^+)$, as −366.9 kcal/mol, in excellent agreement with the experimental thermodynamic values of −367.1 ± 0.2 kcal/mol (based on the NIST gas-phase experimental value[37]) and −366.6 ± 0.1 kcal/mol (based on a very recently revised gas-phase experimental value for $\Delta H_f(OH)$[38,39]). The theoretical values can also be used to predict $\Delta G_{hyd}^{298}(e^-) + \Delta G_{hyd}^{298}(H^+) = -297.9$ kcal/mol and $\Delta G_{hyd}^{298}(e^-) - \Delta G_{hyd}^{298}(HO^-) = 69.0$ kcal/ mol, in excellent agreement with the corresponding values derived from experimental data of −297.8 kcal/mol and of 69.3 ± 0.2 [37] or 68.8 ± 0.1 kcal/mol,[38,39] respectively. On the basis of the success of the SVPE-based supermolecule-continuum calculations for the absolute hydration free energies of the proton, hydroxide ion, and solvated electron, we have used the same computational protocol to predict the energetics of fluoride anion hydration.

In the present study, we first examined various possible stable structures of $F^-(H_2O)_4$ cluster in comparison with the latest experimental data available in the literature. We also explored possible stable structures of larger $F^-(H_2O)_n$ clusters (n = 8, 12, and 16) and their relative thermodynamic properties in both the gas phase and solution. On the basis of the most stable structures, we further predicted the absolute hydration free energies of fluoride anion in the gas-phase clusters and in aqueous solution. The calculated absolute hydration free energy, $\Delta G_{hyd}^{298}(F^-)$, in aqueous solution, together with our calculated of $\Delta G_{hyd}^{298}(H^+)$ are compared with available experimental thermodynamic data.

Computational Methods

The general hybrid supermolecule-continuum approach to the absolute hydration free energy of a charged species has been described elsewhere in detail.[33,34] The physical model for the hybrid supermolecule-continuum approach, i.e., performing a self-consistent reaction field (SCRF) calculation on the supermolecular solute, is that the part of the solvent surrounding the solute is treated quantum mechanically and the remaining bulk solvent is approximated as the dielectric continuum medium.[32] In principle, the more solvent molecules treated quantum mechanically, the better the calculated results. The improvement due to increasing the number of solvent molecules in the supermolecular solute will systematically approach zero in the limit of large n, but this convergence may be very slow. Based on the hybrid supermolecule-continuum approach, the hydration free energy of F^- in water is the free energy of reaction 1, $\Delta G_{hyd}[F^-,n]$, converged to $n \rightarrow \infty$:

$$F^-(gas) + (H_2O)_n(aq) \rightarrow F^-(H_2O)_n(aq) \qquad (1)$$

As in our previous calculations of $\Delta G_{hyd}^{298}(H^+)$ and $\Delta G_{hyd}^{298}(HO^-)$, to calculate the free energy of reaction 1 for $\Delta G_{hyd}^{298}(F^-)$, we need to know the Gibbs free energies of F^-(gas), $(H_2O)_n$(aq), and $F^-(H_2O)_n$(aq). For each of the two aqueous clusters $(H_2O)_n$(aq) and $F^-(H_2O)_n$(aq), the free energy, $G[(H_2O)_n(aq)]$ or $G[F^-(H_2O)_n(aq)]$, can be expressed as a sum of the free energy of the corresponding gas-phase cluster, $(H_2O)_n$(gas) or $F^-(H_2O)_n$(gas), and the bulk solvent shift:

$$G[(H_2O)_n(aq)] = G[(H_2O)_n(gas)] + \Delta G_{sol}[(H_2O)_n] \quad (2)$$

$$G[F^-(H_2O)_n(aq)] = G[F^-(H_2O)_n(gas)] + \Delta G_{sol}[F^-(H_2O)_n] \quad (3)$$

Thus, we can evaluate the hydration free energy of F^- via

$$\Delta G_{hyd}[F^-,n] = \Delta G_{gas}[F^-,n] + \Delta\Delta G_{sol}[F^-,n] \qquad (4)$$

where $\Delta G_{gas}[F^-,n] = G[F^-(H_2O)_n(gas)] - G[(H_2O)_n(gas)] - G[F^-(gas)]$ is the hydration free energy of F^- in gas-phase cluster $F^-(H_2O)_n$ and $\Delta\Delta G_{sol}[F^-,n] = \Delta G_{sol}[F^-(H_2O)_n] - \Delta G_{sol}[(H_2O)_n]$ is the bulk solvent shift of the hydration free energy of F^- from the gas-phase cluster to the solution. At T = 298 K, $\Delta G_{hyd}[F^-,n]$ is converged to $\Delta G_{hyd}^{298}(F^-)$ when $n \rightarrow \infty$. To determine $\Delta G_{hyd}[F^-,n]$ with high accuracy, both $\Delta G_{gas}[F^-,n]$ and $\Delta\Delta G_{sol}[F^-,n]$ must be calculated at a sufficiently high level of theory.

To calculate $\Delta G_{gas}[F^-,n]$ and $\Delta\Delta G_{sol}[F^-,n]$, we first need to optimize geometries of the appropriate structures at a sufficiently high level of theory. Our previous computational studies[33,34] on $\Delta G_{hyd}^{298}(H^+)$ and $\Delta G_{hyd}^{298}(HO^-)$ indicate that geometry optimization of the clusters in the gas phase by using gradient-corrected density functional theory (DFT) with Becke's three-parameter hybrid exchange functional and the Lee−Yang−Parr correlation functional (B3LYP)[40,41,42] in combination with the 6-31++G** basis set[43] is adequate. This level of computation is also adequate for the calculation of the frequencies for use in evaluating the appropriate entropy changes needed to calculate ΔG. Subsequent energy calculations require good treatments of the correlation energy together with very large basis sets. The free energy changes calculated by using geometries

optimized at higher levels, for example, second-order Møller−Plesset (MP2) theory and/or with larger basis sets, were nearly the same as those calculated by using the geometries optimized at the B3LYP/6-31++G** level.[33] The effects of bulk solvent on the optimized geometries are also negligible.[33] Thus, the geometries of $(H_2O)_n$ and $F^-(H_2O)_n$ optimized in the gas phase at the B3LYP/6-31++G** level are appropriate for use in the solvation free energy calculations. The DFT geometry optimizations were followed by analytical second-derivative calculations to ensure that the optimized geometries are minima on the potential energy hypersurface (all real frequencies) and to evaluate the thermal and vibrational corrections to the gas-phase Gibbs free energies (at 298 K and 1 atm). We considered n = 4, 8, 12, and 16 because the structures and energies of neutral water clusters with these n values have already been established in our previous studies.[33,34]

The geometries optimized at the B3LYP/6-31++G** level were then used in single-point energy calculations at the second-order Møller−Plesset (MP2) level with different basis sets including the correlation-consistent basis sets, aug-cc-pVXZ with X = D, T, and Q.[44−47] To extrapolate to the frozen core complete basis set (CBS) limit, we used a three-parameter, mixed exponential/Gaussian function of the form:

$$E(x) = E_{\mathrm{CBS}} + B\exp[-(x-1)] + C\exp[-(x-1)^2] \quad (5)$$

where x = 2, 3, and 4 for aug-cc-pVDZ, aug-cc-pVTZ, and aug-cc-pVQZ, respectively.[46] Additional calculations at the coupled-cluster with single and double substitutions and a noniterative triples correction (CCSD(T))[48−50] level were also done with the correlation-consistent basis sets when possible, as discussed below. We previously showed in our calculations[33] of $\Delta G_{\mathrm{hyd}}^{298}(H^+)$ that the corrections due to core−valence interactions and relativistic effects are small and can be neglected. The overall correction to the electronic energy change due to the core−valence correlation and scalar relativistic effects on $\Delta G_{\mathrm{hyd}}^{298}(H^+)$ is less than 0.1 kcal/mol.[33]

We evaluate the bulk solvent shift, $\Delta\Delta G_{\mathrm{sol}}[F^-,n]$, by performing SCRF calculations on the supermolecular solutes $(H_2O)_n$ and $F^-(H_2O)_n$. The reliability of the SCRF calculation results is dependent on the accuracy of the calculated solvent polarization potential (representing the long-range solute−solvent interaction) in addition to the accuracy of the quantum chemical approximation level for predicting the gas-phase results. Within the continuum model of solvation, the exact solvent electrostatic polarization potential corresponding to a given solute electronic wave function is determined by the solution of the requisite Poisson's equation under a certain boundary condition.[35,51] The full solvent electrostatic polarization consists of both surface and volume polarization.[35] The latter is due to the part of the solute electron charge which quantum mechanically penetrates outside the cavity accommodating the solute. The SVPE procedure described above has been implemented in a local version of the *GAMESS* program[52] to directly determine the volume polarization for an irregularly shaped solute cavity in addition to the more commonly treated surface polarization. In other SCRF implementations, volume polarization effects are ignored or approximately modeled by modifying the surface polarization charge distribution through a simulation and/or charge renormalization,[51,53−60] or the solute charge distribution is simply represented by a set of point charges at the solute nuclei.[61,62]

The SVPE results, converged to the exact solution of Poisson's equation with a given numerical tolerance, depend only on the contour value at a given dielectric constant and on the quantum chemical approach that has been used. A single parameter value of 0.001 au has been determined on the basis of an extensive calibration study using the experimental conformational free energy differences (62 experimental observations) of various polar solutes in various solvents.[35] The SVPE procedure using the 0.001 au contour has been shown to be reliable for evaluating the bulk solvent effects.[32−35] It has also been shown[32,33,35] that the solvent shifts determined by SVPE calculations are rather insensitive to the electron correlation level and basis set used. We have found that there is little difference between the results of the SVPE calculations at the HF/6-31++G** and MP2/6-31++G** levels. Thus for n = 4, we calculated the SVPE contributions to the free energies of solvation at the MP2/6-31++G** level. For the larger clusters with n = 8, 12, and 16, we calculated the SVPE contributions to the free energies of solvation at the HF/6-31++G** level. For the optimal structure in terms of the free energy of solvation for n = 8, 12, and 16, we calculated the final SVPE contributions to the free energies of solvation at the MP2/6-31++G** level as was done for the calculation of the free energies of solvation of the hydroxide anion and other cations.[33,34]

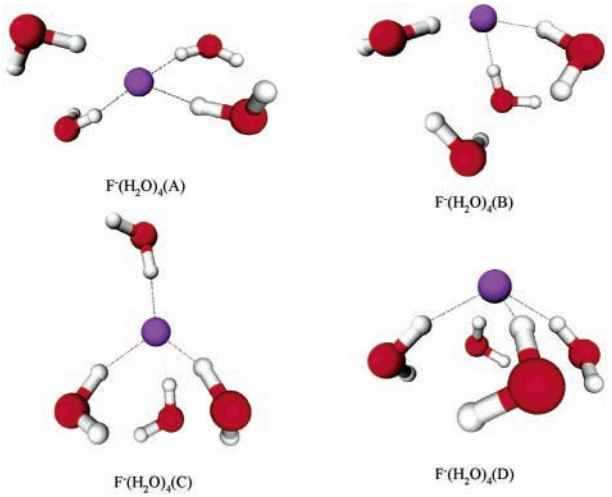

Figure 1. Geometries of the $F^-(H_2O)_4$ cluster optimized at the B3LYP/6-31++G** level.

The Gaussian98 program[63] was used to optimize the geometries and calculate the corresponding vibrational frequencies for most of the cluster structures. The NWChem program[64] was used to optimize the geometries and calculate the corresponding vibrational frequencies of some of the $F^-(H_2O)_{16}$ cluster structures. The MP2 and CCSD(T) energy calculations in the gas phase were performed by using the NWChem and MOLPRO programs.[65] All of the calculations with the NWChem program were carried out on a 256-processor HP Linux Itanium2 Cluster in the Molecular Sciences Computing Facility in the Environmental Molecular Sciences Laboratory, and the calculations with other programs were performed on a 16-processor SGI Origin 2000 computer.

Results and Discussion

Geometries of $F^-(H_2O)_4$. The optimized geometries of four different $F^-(H_2O)_4$ structures are shown in Figure 1. The corresponding Cartesian coordinates are provided as Supporting Information. Structures $F^-(H_2O)_4$(A), $F^-(H_2O)_4$(C), and $F^-(H_2O)_4$(D) each have four F···LHO hydrogen bonds, whereas structure $F^-(H_2O)_4$(B) only has three F^-···HO hydrogen bonds. Four water molecules tetrahedrally coordinate to F^- through

$F^-\cdots HO$ hydrogen bonds in structure $F^-(H_2O)_4$(A). This structure, which only has the C_2 symmetry, slightly deviates from the ideal tetrahedron with D_2 or S_4 symmetry (T_d for the heavy-atom frame). The distortion from the ideal tetrahedral coordination structure comes from the weak attractions between water molecules in each of the two pairs of water molecules: one pair on the left side and the other pair on the right side (Figure 1). For each pair of water molecules, the O···H interaction distance is 2.41 Å, which is not short enough to be considered as a normal O···HO hydrogen bond. The slightly distorted tetrahedral coordination is a result of the balance between the favorable tetrahedral distribution of the four strong $F^-\cdots HO$ hydrogen bonds and the two weak hydrogen bonds between the water molecules. We also optimized the geometries of the two ideal tetrahedral coordination structures, one with D_2 symmetry and the other with S_4 symmetry, and found that both are associated with second-order saddle points on the potential energy surface with each structure having two imaginary vibrational frequencies. The energies of the D_2 and S_4 structures are nearly identical and only ~0.8 kcal/mol higher than the local-minimum C_2 structure, with the energy difference likely due to the weak bonding interactions between the water molecules. With this small energy difference and thermal motions at finite temperatures, one could expect the dynamic average of this structure to be the ideal tetrahedral coordination structure so that the four water molecules in $F^-(H_2O)_4$(A) are dynamically equivalent at most temperatures. This is consistent with the recently reported vibrational spectra suggesting that there are four equivalent water molecules in the $F^-(H_2O)_4$ cluster.[11]

In structure $F^-(H_2O)_4$(C), the F^- is coordinated by three water molecules from one side and by the fourth water molecule from the opposite side. Structure $F^-(H_2O)_4$(D) has a C_4 pyramidal coordination structure, in which water molecules are all on one side. In structure $F^-(H_2O)_4$(B), only three water molecules hydrogen-bond to F^- and the fourth water molecule forms hydrogen bonds with the three water molecules. Structures similar to $F^-(H_2O)_4$(B), $F^-(H_2O)_4$(C), and $F^-(H_2O)_4$(D) have been reported previously by several groups of researchers,[15−21,28] whereas structure $F^-(H_2O)_4$(A) is reported here for the first time. In the past, structure $F^-(H_2O)_4$(C) has been considered to be the most stable one in the gas phase, although structure $F^-(H_2O)_4$(A) was not known.

The calculated Gibbs free energies of the reaction $F^-(g) + (H_2O)_n$(g or aq) → $F^-(H_2O)_n$(g or aq) are summarized in Table 1 for $n = 4$. As shown in Table 1, structure $F^-(H_2O)_4$(C) has a lower free energy than structures $F^-(H_2O)_4$(B) and $F^-(H_2O)_4$(D) in the gas phase at 298 K. However, the free energy of structure $F^-(H_2O)_4$(A) is lower, although the best estimate of the difference is only ~0.7 kcal/mol. The difference of only ~0.7 kcal/mol at 298 K predicts that structures $F^-(H_2O)_4$(A) and $F^-(H_2O)_4$(C) will coexist, with $F^-(H_2O)_4$(A) as the primary component (~80%). This estimate is in the absence of anharmonic contributions to the vibrational modes which could change these energies.

Structural information can also be obtained from comparison of the calculated vibrational frequencies corresponding to the O−H stretches with the experimental frequencies. The frequencies listed in Table 2 are given as the shifts with respect to the mean of the symmetric and asymmetric O−H stretching frequencies in the gas-phase water molecule. The reference frequency given by Cabarcos et al.[16] is 3707 cm^{-1} for the experimental data, the mean of the symmetric and asymmetric stretching frequencies of an isolated H_2O molecule. Our calculation of the vibrational frequencies of H_2O at the B3LYP/6-31++G** level gives 3928 and 3806 cm^{-1} for the symmetric and asymmetric O−H stretching frequencies, respectively, and a reference value for the shifts of 3867 cm^{-1}. The frequency shifts (Table 2) calculated at the B3LYP/6-31++G** level for $F^-(H_2O)_4$(C) are all very close to the corresponding frequency shifts calculated by Cabarcos et al.[16] at the MP/aug-cc-pVDZ level.

TABLE 1: Calculated Gibbs Free Energies (kcal/mol) of Reactions $F^-(g) + (H_2O)_4(g) \rightarrow F^-(H_2O)_4(g)$ and $F^-(g) + (H_2O)_4(aq) \rightarrow F^-(H_2O)_4(aq)$ at $T = 298.15$ K and $P = 1$ atm

	$F^-(H_2O)_4$[a]			
calculation method[b]	A	B	C	D
$F^-(g) + (H_2O)_4(g) \rightarrow F^-(H_2O)_4(g)$				
MP2/aug-cc-pVDZ	−49.1	−46.4	−48.4	−46.0
MP2/aug-cc-pVTZ	−49.7	−47.1	−49.0	−46.4
MP2/aug-cc-pVQZ	−49.7	−46.9	−48.9	−46.2
MP2/CBS	−49.6	−46.7	−48.8	−46.0
CCSD(T)/aug-cc-pVDZ	−50.8	−48.1	−50.2	−48.0
CCSD(T)/aug-cc-pVTZ	−51.3		−50.7	
best estimate[d]	−51.2	−48.4	−50.5	−48.0
bulk solvent shift[c]	−45.2	−45.1	−42.5	−42.3
$F^-(g) + (H_2O)_4(aq) \rightarrow F^-(H_2O)_4(aq)$				
MP2/aug-cc-pVDZ	−94.3	−91.5	−90.8	−88.3
MP2/aug-cc-pVTZ	−94.9	−92.2	−91.5	−88.6
MP2/aug-cc-pVQZ	−94.9	−92.0	−91.4	−88.4
MP2/CBS	−94.8	−91.8	−91.3	−88.3
CCSD(T)/aug-cc-pVDZ	−96.0	−93.1	−92.7	−90.3
CCSD(T)/aug-cc-pVTZ	−96.5		−93.2	
best estimate[d]	−96.4	−93.4	−93.0	−90.3

[a] For structure labels see Figure 1. [b] Method for energy calculations in the gas phase. All energy calculations were performed by using geometries optimized at the B3LYP/6-31++G** level. [c] Calculated by performing SVPE calculations at the MP2/6-31++G** level. [d] The best estimate is the MP2/CBS value plus the higher order electron correlation correction estimated as the energy shift from the MP2/aug-cc-pVTZ value to the corresponding CCSD(T)/aug-cc-pVTZ value or from the MP2/aug-cc-pVDZ value to the corresponding CCSD(T)/aug-cc-pVDZ value.

As shown in Table 2, the frequency shifts and intensities calculated for $F^-(H_2O)_4$(B) and $F^-(H_2O)_4$(D) are not in agreement with the three measured frequency shifts at −638, −348, and −7 cm^{-1}. The observed frequency shifts most likely correspond to the vibration modes with the highest intensities. The frequency shifts and intensities calculated for both $F^-(H_2O)_4$(A) and $F^-(H_2O)_4$(C) are in reasonable agreement with the three measured experimental frequencies. For $F^-(H_2O)_4$(A), the calculated frequency shifts at −700, −370, and −52 cm^{-1} with strong intensities match well with the experimental shifts at −638, −348, and −7 cm^{-1}, respectively;[16] the corresponding deviations are −62, −22, and −45 cm^{-1}. For $F^-(H_2O)_4$(C), the calculated shifts at −598 and −373 cm^{-1} are close to the experimental shifts at −638 and −348 cm^{-1}, respectively, and the third experimental frequency shift at −7 cm^{-1} should be associated with the average of the three theoretical shifts at −58, −54, and −47 cm^{-1}; the corresponding deviations from the three experimental shifts are +40, −25, and ~−46 cm^{-1}. On the basis of the comparison in the vibrational frequency shifts, structures $F^-(H_2O)_4$(B) and $F^-(H_2O)_4$(D) can be excluded from the candidates of the most stable structure of $F^-(H_2O)_4$ in the gas phase. It is harder to differentiate which of the shifts for $F^-(H_2O)_4$(A) or $F^-(H_2O)_4$(C) are closer to the observed IR spectra shifts of $F^-(H_2O)_4$.

It is well-established that the calculated vibrational frequencies systematically deviate from the experimental frequencies due to anharmonic effects and the level of the computation.

TABLE 2: Calculated Vibrational Frequencies (ω, cm^{-1}) and Vertical Electron Detachment Energies (VDE, eV) of $F^-(H_2O)_4$ Clusters in the Gas Phase Compared with the Corresponding Experimental Data

	calculated at the B3LYP/6-31++G** level[a]							
expt	A		B		C		D	
$\Delta\omega$[b]	$\Delta\omega$[b]	intensity	$\Delta\omega$[b]	intensity	$\Delta\omega$[b]	intensity	$\Delta\omega$[b]	intensity
−638	−700	1990	−1009	1480	−598	1747	−487	0
	−628	269	−754	799	−489	341	−474	746
−348	−370	1100	−391	510	−478	303	−474	746
	−324	47	−291	305	−373	600	−349	654
−7	−52	105	−230	531	−58	73	−60	95
	−51	31	−118	179	−54	56	−58	90
	10	44	−29	31	−47	51	−58	90
	11	0	9	17	10	19	−55	0
				VDE				
7.35 ± 0.20[c]	6.08 (7.81[d])		6.21		5.48 (7.83[d])		6.30	

[a] For structure labels see Figure 1. Unless indicated, all calculations were performed at the B3LYP/6-31++G** level. [b] Experimental data from ref 16. All of the vibrational frequencies are given as shifts with respect to the corresponding mean of the symmetric and asymmetric O−H stretches in the gas-phase water molecule (3707 cm^{-1} for experiment and 3867 cm^{-1} for the B3LYP/6-31++G** calculations). [c] Experimental VDE from ref 22. [d] The values in parentheses were calculated at the MP2/aug-cc-pVTZ level.

The calculated frequency shifts listed in Table 2 are given without scaling. The calculated harmonic vibrational frequencies are usually systematically higher than the corresponding experimental frequencies. The calculated frequencies usually need to be scaled down to better reproduce the corresponding experimental frequencies. The values of this empirical scaling factor (SF) used in the literature are generally smaller than unity, and the optimal value is dependent on the calculation method. For example, it has been suggested[66] that SF = 0.8929 at the HF/6-31G* level and SF = 0.9613 for the B3LYP/6-31G* level. We can estimate an optimal SF value for our calculations at the B3LYP/6-31++G** level. The theoretical reference frequency of 3867 cm^{-1} is higher than the experimental reference frequency of 3707 cm^{-1} by 160 cm^{-1}, suggesting that the calculations at the B3LYP/6-31++G** level indeed overestimate the vibrational frequencies. The ratio of the experimental reference frequency value to the theoretical reference frequency value gives SF = 0.9586. By using this SF, the calculated frequency shifts −700, −370, and −52 cm^{-1} calculated for $F^-(H_2O)_4$(A) scale to −671, −355, and −50 cm^{-1}, respectively, whereas the frequency shifts −598, −373, and ∼−53 cm^{-1} calculated for $F^-(H_2O)_4$(C) scale to −573, −358, and ∼−51 cm^{-1}, respectively. The deviations of the scaled theoretical frequency shifts from the experimental shifts[16] of −638, −348, and −7 cm^{-1} are −33, −7, and −43 cm^{-1}, respectively, for $F^-(H_2O)_4$(A) and +65, −10, and −44 cm^{-1}, respectively, for $F^-(H_2O)_4$(C). The use of the scaling factor makes the calculated shifts for $F^-(H_2O)_4$(A) in slightly better agreement with those for $F^-(H_2O)_4$(C), but we cannot conclusively state that structure A is the correct structure based on this analysis.

The calculated vertical electron detachment energies (VDE's) are compared with the experimental VDE value of 7.35 ± 0.20 eV [22] in Table 2. The VDE value, 6.08 eV, calculated for the most stable structure, $F^-(H_2O)_4$(A), at the B3LYP/6-31++G** level is smaller than the experimental value by over 1 eV. The VDE values for structure A calculated at the MP2/aug-cc-pVDZ, MP2/aug-cc-pVTZ, and MP2/aug-cc-pVQZ levels are 7.67, 7.81, and 7.88 eV, respectively, giving an MP2/CBS value of 7.92 eV. The MP2/CBS value is larger than the experimental VDE value by ∼0.6 eV. The VDE values calculated at the B3LYP/6-31++G** level for $F^-(H_2O)_4$(B) and $F^-(H_2O)_4$(D) are close to that calculated for $F^-(H_2O)_4$(A) at the same level, and that for structure C is smaller. We calculated the VDE for structure C at the MP2/aug-cc-pVDZ and MP2/aug-cc-pVTZ levels. The results at the MP2 level are very similar to those for structure A with an MP2/aug-cc-pVDZ value of 7.69 eV and an MP2/aug-cc-pVTZ value of 7.83 eV for VDE-($F^-(H_2O)_4$(C)). The calculations are only in qualitative agreement with experiment, and higher correlation treatment levels are needed to obtain better agreement. Furthermore, the VDE calculations in combination with the photoelectron spectroscopy experiment do not allow us to distinguish between the different $F^-(H_2O)_4$ structures. Such calculations are beyond the scope of this work in terms of the free energy of solvation of F^-.

The energetic results in Table 1 show that bulk solvent effects differentially stabilize the $F^-(H_2O)_4$ structures. The calculated bulk solvent shifts of the hydration free energies of F^- in $F^-(H_2O)_4$(A) and $F^-(H_2O)_4$(B) are larger than those in $F^-(H_2O)_4$(C) and $F^-(H_2O)_4$(D) by ∼3 kcal/mol. The bulk solvent effects most favorably stabilize structure $F^-(H_2O)_4$(A) so that the free energy difference between this most stable structure and that of the second most stable becomes as large as ∼3.0 kcal/mol in aqueous solution, as compared to a difference of only 0.7 kcal/mol in the gas phase.

Geometries of $F^-(H_2O)_n$ (n = 8, 12, and 16). The optimized geometries of the $F^-(H_2O)_n$ clusters (n = 8, 12, and 16) are shown in Figures 2−4 and the corresponding energetic results are summarized in Tables 3−5. All of these structures are reported for the first time as far as we are aware.

Structure $F^-(H_2O)_8$(A) (Figure 2) is similar to the most stable structure of $HO^-(H_2O)_8$ in terms of hydrogen bonding. In $F^-(H_2O)_8$(A), four water molecules coordinate to F^- and the other four water molecules form a four-water ring hydrogen-bonded to the first four water molecules. $F^-(H_2O)_8$(A) corresponds to the pyramidal $F^-(H_2O)_4$(D) structure if the four-water ring is removed consistent with a surface state. $F^-(H_2O)_8$(B) can be built from the pyramidal $F^-(H_2O)_4$(D) structure with each of the four additional water molecules linked to two neighboring water molecules coordinating to F^-. $F^-(H_2O)_8$(C) can be constructed from the tetrahedrally coordinated $F^-(H_2O)_4$(A) structure with each of four additional water molecules hydrogen-bonding to two water molecules coordinated to F^- on one side. DFT calculations at the B3LYP/6-31++G** level led to two small imaginary vibrational frequencies (10i and 4i cm^{-1}). The two small imaginary frequencies are likely due to the inaccuracy of the numerical calculation at the DFT level.[67] We note that DFT calculations on $F^-(H_2O)_8$(C) at the B3LYP/6-31+G* level gave only one small imaginary frequency of 9i cm^{-1}. We also optimized the geometry of another $F^-(H_2O)_8$ structure (with the D_4 symmetry) in which eight water molecules all equivalently

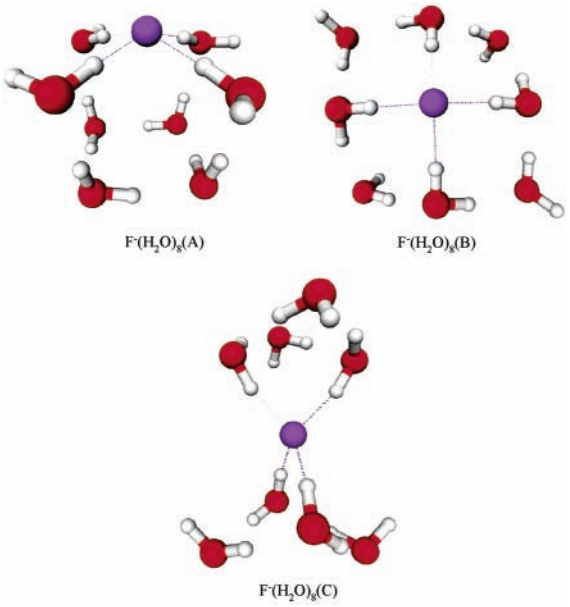

Figure 2. Geometries of the $F^-(H_2O)_8$ cluster optimized at the B3LYP/6-31++G** level.

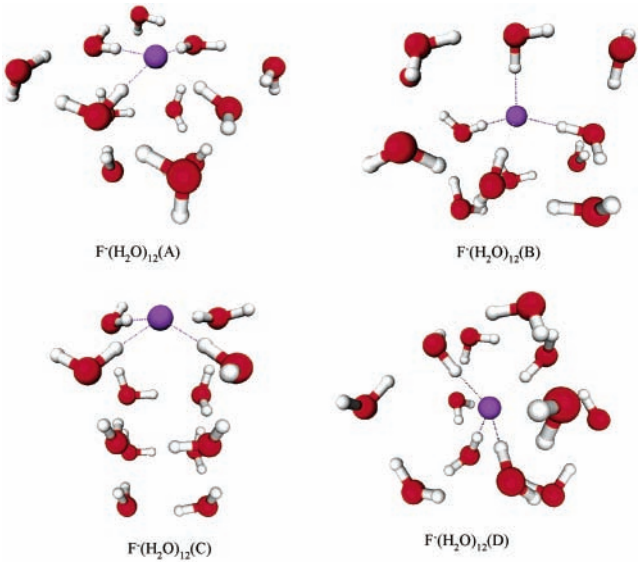

Figure 3. Geometries of the $F^-(H_2O)_{12}$ cluster optimized at the B3LYP/6-31++G** level.

coordinate to F^-: four water molecules coordinate to F^- from one side and the other four water molecules from another side. The D_4 structure is associated with a sixth-order saddle point on the potential energy surface with six calculated imaginary frequencies between 124*i* and 30*i* cm^{-1}. As shown in Table 3, the most stable structure for $n = 8$ is $F^-(H_2O)_8$(A) in both the gas phase and solution.

$F^-(H_2O)_{12}$(A) (Figure 3) is constructed from $F^-(H_2O)_8$(B) plus a four-water ring that forms hydrogen bonds with the four water molecules coordinating to F^-. $F^-(H_2O)_{12}$(B) is constructed from $F^-(H_2O)_4$(C) plus eight water molecules forming a hydrogen-bonding network with the four water molecules in the first solvation shell. $F^-(H_2O)_{12}$(C) is constructed from $F^-(H_2O)_8$(A) plus a four-water ring forming hydrogen bonds with another four-water ring. $F^-(H_2O)_{12}$(D) with D_2 symmetry is constructed from $F^-(H_2O)_8$(C) plus four bridging water molecules linking a water molecule on one side to a water molecule on the other side; we note that in $F^-(H_2O)_8$(C) there are four water molecules on each of the two sides (up and down). As shown in Table 4, the most stable structure for $n = 12$ in the gas phase is $F^-(H_2O)_{12}$(C), whereas $F^-(H_2O)_{12}$(A) is the most stable one in solution. The bulk solvent effects can significantly change the relative stability of the $F^-(H_2O)_{12}$ structures.

$F^-(H_2O)_{16}$(A) (Figure 4) is constructed from $F^-(H_2O)_{12}$(D) plus four water molecules, each forming hydrogen bonds with the other three water molecules. $F^-(H_2O)_{16}$(B) with D_2 symmetry is constructed from $F^-(H_2O)_8$(C) plus four pairs of water molecules. Each of these pairs of water molecules is a bridge linking a water molecule on one side to a water molecule on the other side. The essential difference between $F^-(H_2O)_{16}$(B) and $F^-(H_2O)_{12}$(D) is that each of the four bridging water molecules in $F^-(H_2O)_{12}$(D) is replaced by a pair of hydrogen-bonded water molecules such that the hydrogen-bond network becomes relatively more relaxed in $F^-(H_2O)_{16}$(B). $F^-(H_2O)_{16}$(C) can be considered to be a structure formed from $F^-(H_2O)_{12}$(C) plus an additional four-water ring hydrogen-bonding to the other four-water ring on the down side. $F^-(H_2O)_{16}$(D) is constructed from $F^-(H_2O)_{12}$(A) plus an additional four-water ring hydrogen-bonding to the four-water ring in $F^-(H_2O)_{12}$(A). $F^-(H_2O)_{16}$(E) is constructed from $F^-(H_2O)_8$(B) plus an eight-water ring hydrogen-bonding to the eight water molecules in $F^-(H_2O)_8$(B). As shown in Table 5, structure $F^-(H_2O)_{16}$(D) has the lowest free energy in the gas phase, whereas $F^-(H_2O)_{16}$(A) has the lowest free energy in aqueous solution. Structure $F^-(H_2O)_{16}$(B) has the highest free energy in the gas phase but has the second lowest free energy in solution, further demonstrating the importance of bulk solvent effects on the relative stability of the cluster structures.

An important trend in the relative stabilities of the hydration structures is that in both gas phase and solution, from $n = 8$ to $n = 12$ and to $n = 16$, the tetrahedrally coordinated fluoride anion hydration structure becomes more and more stable as compared to the other hydration structures with pyramidal coordination of water molecules to F^-. For $n = 8$, the free energy of the tetrahedrally coordinated fluoride anion hydration structure $F^-(H_2O)_8$(C) is higher than that of the most stable structure $F^-(H_2O)_8$(A) by ~6 kcal/mol in the gas phase and by ~15 kcal/mol in solution. For $n = 12$, the free energy of the tetrahedrally coordinated fluoride anion hydration structure $F^-(H_2O)_{12}$(D) is higher than that of the most stable structure $F^-(H_2O)_{12}$(C) by ~4 kcal/mol in the gas phase and higher than that of the most stable structure $F^-(H_2O)_{12}$(A) by ~4 kcal/mol in solution. For $n = 16$, the free energy of the tetrahedrally coordinated fluoride anion hydration structure $F^-(H_2O)_{16}$(A) is higher than that of the most stable structure $F^-(H_2O)_{16}$(D) by ~3 to 4 kcal/mol in the gas phase, but $F^-(H_2O)_{16}$(A) becomes the most stable structure in solution. Another tetrahedrally coordinated fluoride anion hydration structure, $F^-(H_2O)_{16}$(B), is the second most stable one in solution.

This general trend can be understood by the observation that the stability of a hydration structure is a result of the balance between $F^-\cdots$HO hydrogen bonding and O$\cdots$HO hydrogen bonding in a $F^-(H_2O)_n$ cluster. An ideal hydration structure not only tends to form four strong $F^-\cdots$HO hydrogen bonds with a tetrahedral geometry but also tends to keep the O$\cdots$HO hydrogen bonds between water molecules as much as possible. For $n = 4$, an $F^-(H_2O)_4$ cluster can either have four strong $F^-\cdots$HO hydrogen bonds or have less strong $F^-\cdots$HO hydrogen bonds plus some O$\cdots$HO hydrogen bonds between the water molecules. The total strength of the tetrahedrally distributed four $F^-\cdots$HO hydrogen bonds is stronger than that of three $F^-\cdots$HO hydrogen bonds plus three O$\cdots$HO hydrogen bonds, and the

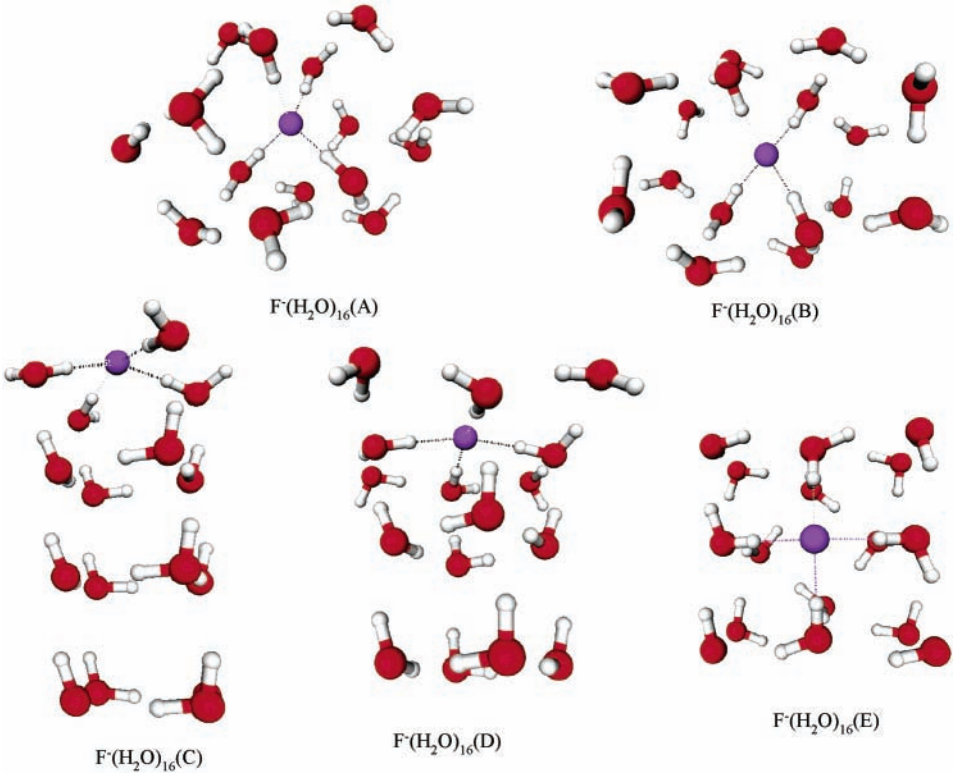

Figure 4. Geometries of the $F^-(H_2O)_{16}$ cluster optimized at the B3LYP/6-31++G** level.

TABLE 3: Calculated Gibbs Free Energies (kcal/mol) of Reactions $F^-(g) + (H_2O)_8(g) \rightarrow F^-(H_2O)_8(g)$ and $F^-(g) + (H_2O)_8(aq) \rightarrow F^-(H_2O)_8(aq)$ at $T = 298.15$ K and $P = 1$ atm

	$F^-(H_2O)_8$[a]		
calculation method[b]	A	B	C
$F^-(g) + (H_2O)_8(g) \rightarrow F^-(H_2O)_8(g)$			
MP2/aug-cc-pVDZ	−57.7	−55.1	−55.3
MP2/aug-cc-pVTZ	−58.6	−56.5	−56.5
MP2/aug-cc-pVQZ	−58.6		
MP2/CBS	−58.6		
CCSD(T)/aug-cc-pVDZ	−59.7		
best estimate[d]	−60.6		
bulk solvent shift[c]	−42.1	−37.5	−36.0
$F^-(gas) + (H_2O)_4(aq) \rightarrow F^-(H_2O)_4(aq)$			
MP2/aug-cc-pVDZ	−99.8	−92.6	−84.0
MP2/aug-cc-pVTZ	−100.7	−94.0	−85.3
MP2/aug-cc-pVQZ	−100.7		
MP2/CBS	−100.7		
CCSD(T)/aug-cc-pVDZ	−101.8		
best estimate[d]	−102.7		

[a] For structure labels see Figure 2. [b] Method for the energy calculations in the gas phase. All energy calculations were performed by using geometries optimized at the B3LYP/6-31++G** level. [c] Calculated by performing the SVPE calculations at the HF/6-31++G** level. [d] The best estimate is the MP2/CBS value plus the higher order electron correlation correction estimated as the energy shift from the MP2/aug-cc-pVDZ value to the corresponding CCSD(T)/aug-cc-pVDZ value.

TABLE 4: Calculated Gibbs Free Energies (kcal/mol) of Reactions $F^-(g) + (H_2O)_{12}(g) \rightarrow F^-(H_2O)_{12}(g)$ and $F^-(g) + (H_2O)_{12}(aq) \rightarrow F^-(H_2O)_{12}(aq)$ at $T = 298.15$ K and $P = 1$ atm

	$F^-(H_2O)_{12}$[a]			
calculation method[b]	A	B	C	D
$F^-(g) + (H_2O)_{12}(g) \rightarrow F^-(H_2O)_{12}(g)$				
MP2/aug-cc-pVDZ	−63.8	−60.8	−65.1	−60.7
MP2/aug-cc-pVTZ	−64.8	−62.0	−65.8	−61.6
MP2/aug-cc-pVQZ	−64.8		−65.8	
MP2/CBS	−64.7		−65.8	
bulk solvent shift[c]	−38.6	−40.9	−35.7	−38.0
$F^-(g) + (H_2O)_{12}(aq) \rightarrow F^-(H_2O)_{12}(aq)$				
MP2/aug-cc-pVDZ	−102.5	−101.7	−100.8	−98.7
MP2/aug-cc-pVTZ	−103.5	−102.9	−101.5	−99.6
MP2/aug-cc-pVQZ	−103.4		−101.5	
MP2/CBS	−103.3		−101.5	

[a] For structure labels see Figure 3. [b] Method for the energy calculations in the gas phase. All energy calculations were performed by using geometries optimized at the B3LYP/6-31++G** level. [c] Calculated by performing the SVPE calculations at the HF/6-31++G** level.

tetrahedrally coordinated fluoride anion hydration structure is the most stable. For $n = 8$, an $F^-(H_2O)_8$ cluster can have both $F^-\cdots$HO and O$\cdots$HO hydrogen bonds as the number of water molecules is larger than the required number of water molecules to form the first solvation shell. The tetrahedrally coordinated fluoride anion hydration structure, $F^-(H_2O)_8$(C), has four hydrogen-bonded water molecules each above and below, and there is no hydrogen bonding between the two sides. All of the water molecules can only form a single hydrogen-bonded network and, therefore, structure $F^-(H_2O)_8$(C) is less stable than the other two $F^-(H_2O)_8$ structures. With further increasing n, more and more water molecules can be used as bridges linking the water molecules on the two sides of the $F^-(H_2O)_8$(C) core structure through O$\cdots$HO hydrogen bonds so that the tetrahedrally coordinated fluoride anion hydration structure becomes more and more stable.

An important implication of the trend of the relative stability change for $F^-(H_2O)_n$ cluster structures in the gas phase is that, with increasing n, fluoride anion will eventually become internally solvated even in the gas-phase $F^-(H_2O)_n$ cluster. The same trend may be found for other hydrated anion clusters. This provides insight into the transition from hydration structures for small gas-phase hydrated anion clusters to aqueous solution.

TABLE 5: Calculated Gibbs Free Energies (kcal/mol) of Reactions $F^-(g) + (H_2O)_{16}(g) \rightarrow F^-(H_2O)_{16}(g)$ and $F^-(g) + (H_2O)_{16}(aq) \rightarrow F^-(H_2O)_{16}(aq)$ at $T = 298.15$ K and $P = 1$ atm

	$F^-(H_2O)_{16}$[a]				
calculation method[b]	A	B	C	D	E
$F^-(g) + (H_2O)_{16}(g) \rightarrow F^-(H_2O)_{16}(g)$					
MP2/aug-cc-pVDZ	−65.2	−60.3	−68.5	−68.5	−67.3
MP2/aug-cc-pVTZ	−66.1	−62.4	−69.2	−69.6	−67.9
bulk solvent shift[c]	−37.3	−37.9	−30.5	−28.7	−28.3
$F^-(g) + (H_2O)_{16}(aq) \rightarrow F^-(H_2O)_{16}(aq)$					
MP2/aug-cc-pVDZ	−102.4	−98.2	−99.1	−97.2	−95.6
MP2/aug-cc-pVTZ	−103.3	−100.2	−99.7	−98.3	−96.2

[a] For structure labels see Figure 4. [b] Method for the energy calculations in the gas phase. All energy calculations were performed by using geometries optimized at the B3LYP/6-31++G** level. [c] Calculated by performing the SVPE calculations at the HF/6-31++G** level.

TABLE 6: Absolute Hydration Free Energy of F^- (kcal/mol) Calculated as the Converged Free Energy Change from $F^-(g) + (H_2O)_n(aq) \rightarrow F^-(H_2O)_n(aq)$ at $T = 298.15$ K and $P = 1$ atm

	Gibbs free energy change			
calculation method[a]	$n = 4$	$n = 8$	$n = 12$	$n = 16$
bulk solvent shift (i.e., $\Delta\Delta G_{sol}[F^-,n]$)[b]	-45.2	-41.8	-38.3	-36.7
including bulk solvent shift (i.e., $\Delta G_{hyd}[F^-,n]$)				
MP2/aug-cc-pVDZ	−94.3	−99.5	−102.1	−101.9
MP2/aug-cc-pVTZ	−94.9	−100.4	−103.1	−102.8
MP2/aug-cc-pVQZ	−94.9	−100.4	−103.1	(−102.8)[d]
MP2/CBS	−94.8	−100.4	−103.0	(−102.7)[d]
CCSD(T)/aug-cc-pVDZ	−96.0	−101.5		
CCSD(T)/aug-cc-pVTZ	−96.5			
best estimate[c]	−96.4	−102.4	-104.6 ± 0.4	-104.3 ± 0.4

[a] Method for the energy calculations in the gas phase. All energy calculations were performed by using geometries optimized at the B3LYP/6-31++G** level. [b] Calculated by performing the SVPE calculations at the MP2/6-31++G** level. [c] The best estimate is the MP2/CBS value plus the higher order electron correlation correction estimated as the energy shift from the MP2/aug-cc-pVTZ value to the corresponding CCSD(T)/aug-cc-pVTZ value for $n = 4$ (∼−1.6 kcal/mol) or from the MP2/aug-cc-pVDZ value to the corresponding CCSD(T)/aug-cc-pVDZ value for $n = 8$ (∼−2.0 kcal/mol). For $n = 12$ and 16, the energy shift is estimated to be -1.6 ± 0.4 kcal/ mol. [d] Estimated on the basis of the constant shift of the results from MP2/aug-cc-pVTZ to MP2/aug-cc-pVQZ and to MP2/CBS for $n = 4$, 8, and 12.

Hydration Free Energies. The hydration free energies of F^-, $\Delta G_{gas}[F^-,n]$ defined as the free energy of reaction $F^-(gas) + (H_2O)_n(gas) \rightarrow F^-(H_2O)_n(gas)$, in all of the calculated gas-phase $F^-(H_2O)_n$ clusters are summarized in Tables 1 and 3−5. For $n = 4$, the SVPE contributions to the free energies of solvation were calculated at the MP2/6-31++G** level and for $n = 8$, 12, and 16 at the HF/6-31++G** level. The corresponding hydration free energies of F^-, $\Delta G_{hyd}[F^-,n]$, calculated as the free energy of reaction $F^-(gas) + (H_2O)_n(aq) \rightarrow F^-(H_2O)_n(aq)$, are also listed in the tables. The $\Delta G_{hyd}[F^-,n]$ values calculated for $n = 4$, 8, 12, and 16 for the most stable $F^-(H_2O)_n$ structures in solution are summarized in Table 6. For the results in Table 6, the SVPE contributions to the free energies of solvation were calculated at the MP2/6-31++G** level for all n. The standard state used to obtain the values listed in the tables is the hypothetical ideal gas existing at $T = 298$ K and $P = 1$ atm, which gives a density of 1/24.465 mol/L. The standard state is 1 mol/L in solution at $T = 298$ K and $P = 1$ atm.

The convergence of the calculated hydration free energy with respect to n is shown in Table 6. There is a large change, ∼6 kcal/mol, in the calculated hydration free energy from $n = 4$ to $n = 8$. The change in hydration free energy from $n = 8$ to $n = 12$ is ∼2 kcal/mol. The change from $n = 12$ to $n = 16$ is smaller than ∼0.3 kcal/mol, and we suggest that the $\Delta G_{hyd}[F^-,n]$ calculation is well-converged at $n = 12$ or 16.

Because the hydration free energy calculations are well-converged at $n = 12$ or 16 for solvated F^-, we just need to perform as high-level energy calculations as possible on the aqueous clusters up to $n = 12$ or 16. The CCSD(T) method can predict total molecular dissociation energies involving covalent bonds based on the valence electrons to within tenth-(s) of a kilocalorie per mole[38,68,69] when a sufficiently large basis set is used and extrapolated to the complete basis set limit and if other effects such as core−valence correlation, relativity, and zero-point energies are properly accounted for. The MP2 method has been shown to give very good energies for hydrogen-bonded systems.[70−72] We extrapolate the MP2 energies to the CBS limit by using the augmented correlation-consistent basis sets, aug-cc-pVDZ, aug-cc-pVTZ, and aug-cc-pVQZ, with eq 5. The MP2/CBS results lead to $\Delta G_{hyd}[F^-,4] = -94.8$ kcal/mol, $\Delta G_{hyd}[F^-,8] = -100.4$ kcal/mol, and $\Delta G_{hyd}[F^-,12] = -103.0$ kcal/mol. We were unable to complete a MP2/aug-cc-pVQZ calculation on $F^-(H_2O)_{16}$(A). The results obtained for $n = 4$, 8, and 12 suggest that the $\Delta G_{hyd}[F^-,n]$ value calculated at the MP2/aug-cc-pVQZ level should be nearly identical to the value at the MP2/aug-cc-pVTZ level and that the MP2/CBS value is only smaller than the MP2/aug-cc-pVTZ and MP2/aug-cc-pVQZ values by ∼0.1 kcal/mol. Thus, it is reasonable to estimate that $\Delta G_{hyd}[F^-,16] = -102.8$ and −102.7 kcal/mol at the MP2/aug-cc-pVQZ and MP2/CBS levels, respectively.

We were unable to complete CCSD(T) energy calculations on $F^-(H_2O)_{12}$(A) and $F^-(H_2O)_{16}$(A) using the augmented correlation-consistent basis sets due to hardware and software limitations, but we were able to carry out the CCSD(T) energy calculations on $F^-(H_2O)_8$(A) with the aug-cc-pVDZ basis set and on all of the $F^-(H_2O)_4$ structures with the aug-cc-pVTZ or/and aug-cc-pVDZ basis sets. The hydration free energy shifts from the MP2 calculations to the corresponding CCSD(T) calculations are all between −1.6 and −2.0 kcal/mol. The shift

of −1.6 kcal/mol is for the tetrahedrally coordinated fluoride anion hydration structure, $F^-(H_2O)_4$(A). So, for the tetrahedrally coordinated fluoride anion hydration structure $F^-(H_2O)_{16}$(A), as well as $F^-(H_2O)_{16}$(A), the hydration free energy shifts from the MP2 to the CCSD(T) are estimated to be close to -1.6 ± 0.4 kcal/mol. Thus we obtain our best estimates for $n = 12$ and 16 as $\Delta G_{hyd}[F^-,12] = -104.6 \pm 0.4$ kcal/mol and $\Delta G_{hyd}[F^-,16] = -104.3 \pm 0.4$ kcal/mol, in comparison with the best estimates of $\Delta G_{hyd}[F^-,4] = -96.4$ kcal/mol and $\Delta G_{hyd}[F^-,8] = -102.4$ kcal/mol. Thus, our best estimate of the absolute hydration free energy of F^-, $\Delta G_{hyd}^{298}(F^-)$, is -104.3 ± 0.7 kcal/mol for the above-defined standard states. Our predicted $\Delta G_{hyd}^{298}(F^-)$ value is ~4.4 kcal/mol more negative than the value of −99.9 kcal/mol calculated by Topol et al. with $n = 6$ (their largest n value).[28] In addition, their result is dependent on the radius used for F^- in their solvation calculations in addition to the issues of other empirical parameters and ab initio calculations at the relatively lower levels. We note that their value for $n = 6$ falls between our values for $n = 4$ and $n = 8$, as would be expected.

How can the accuracy of our prediction for $\Delta G_{hyd}^{298}(F^-)$ be tested? Recently, the absolute hydration free energy of F^-, $\Delta G_{hyd}^{298}(F^-)$, was derived to be −105.0 kcal/mol by Pliego and Riveros[73] from the combined use of thermodynamic properties (including the pK_a and gas-phase basicity, etc.) and a $\Delta G_{hyd}^{298}(H^+)$ value of −264.0 kcal/mol. Our $\Delta G_{hyd}^{298}(F^-)$ value of -104.3 ± 0.7 kcal/mol is in excellent agreement with the value of −105.0 kcal/mol by Pliego and Riveros. The predicted $\Delta G_{hyd}^{298}(F^-)$ value of -104.3 ± 0.7 kcal/mol combined with our previously predicted $\Delta G_{hyd}^{298}(H^+)$ value of −262.4 kcal/mol [33] gives $\Delta G_{hyd}^{298}(F^-) + \Delta G_{hyd}^{298}(H^+) = -366.7 \pm 0.7$ kcal/mol. The predicted $\Delta G_{hyd}^{298}(F^-) + \Delta G_{hyd}^{298}(H^+)$ value can be tested by an appropriate combination of well-established experimental thermodynamic data collected by Tissandier et al.[26] Tissandier et al. concluded that the experimental $\Delta G_{hyd}^{298}(F^-) + \Delta G_{hyd}^{298}(H^+)$ value should be −366.5 kcal/mol,[26] in excellent agreement with our predicted $\Delta G_{hyd}^{298}(F^-) + \Delta G_{hyd}^{298}(H^+)$ value of -366.7 ± 0.7 kcal/mol. Such excellent agreement strongly suggests that our calculated value for $\Delta G_{hyd}^{298}(F^-)$ is reliable.

Conclusion

A series of first-principles electronic structure calculations have been performed to determine the most stable structures of $F^-(H_2O)_n$ clusters ($n = 4$, 8, 12, and 16) and to determine the corresponding absolute hydration free energies of fluoride anion (F^-) in the gas-phase clusters and in aqueous solution. The calculated results indicate that in both the gas phase and solution, when $n = 4$ at $T = 298$ K, a tetrahedrally coordinated fluoride anion hydration structure is lower in Gibbs free energy than the structure which has been considered to be the most stable structure of $F^-(H_2O)_4$ cluster in the gas phase. Likely candidates for the most stable hydration structures of $F^-(H_2O)_n$ clusters ($n = 8$, 12, and 16) have also been predicted on the basis of ab initio electronic structure calculations. The calculated results indicate that the bulk solvent effects can qualitatively change the relative thermodynamic stability of the different possible structures of $F^-(H_2O)_n$ clusters and that the most stable structure in solution is not necessarily the most stable structure in the gas phase. For example, the lowest free energy structure of $F^-(H_2O)_{16}$ is associated with a hydration structure having pyramidal coordination of F^- in the gas phase and with a hydration structure having tetrahedral coordination in aqueous solution.

The energetic results reveal an important trend in terms of the change of the relative stability of the hydration structures from $n = 8$ to $n = 12$ to $n = 16$. The tetrahedrally coordinated fluoride anion hydration structure becomes more stable as compared to the other hydration structures with pyramidal coordination. This trend can be understood on the basis of the observation that a hydration structure is a result of the balance between F^-LHO hydrogen bonds and the OLHO hydrogen bonds in the cluster. This leads to the conclusion that, with increasing numbers of water molecules, the fluoride anion will eventually become internally solvated even in a gas-phase $F^-(H_2O)_n$ cluster. The same trend may be found for other hydrated anion clusters.

Based on the most stable structures, the absolute hydration free energy of fluoride anion in aqueous solution, $\Delta G_{hyd}^{298}(F^-)$, is predicted to be -104.3 ± 0.7 kcal/mol by using a reliable computational protocol of first-principles solvation-included electronic structure calculations, the same approach recently used to calculate the absolute hydration free energies of the proton and other charged particles. The predicted values of the $\Delta G_{hyd}^{298}(F^-)$ value combined with our previously predicted $\Delta G_{hyd}^{298}(H^+)$ value of −262.4 kcal/mol gives $\Delta G_{hyd}^{298}(F^-) + \Delta G_{hyd}^{298}(H^+) = -366.7 \pm 0.7$ kcal/mol in excellent agreement with the value of −366.5 kcal/mol derived from available experimental data.

Acknowledgment. This work was supported in part by PNNL Laboratory Directed Research and Development funds. Part of this work was done using the Molecular Sciences Computing Facility (MSCF) in the William R. Wiley Environmental Molecular Sciences Laboratory (EMSL) at the Pacific Northwest National Laboratory. The EMSL including the MSCF is a national user facility funded by the Office of Biological and Environmental Research of the U.S. Department of Energy. PNNL is a multiprogram national laboratory operated by Battelle Memorial Institute for the U.S. Department of Energy.

Supporting Information Available: The optimized geometries of the anionic cluster structures and the corresponding energies, zero-point vibration energies, dipole moments, and quadrupole moments. This material is available free of charge via the Internet at http://pubs.acs.org.

References and Notes

(1) Conway, B. E. *Ionic Hydration in Chemistry and Biophysics*; Elsevier: New York, 1981.
(2) Marcus, Y. *Ion Solvation*; Wiley: New York, 1985.
(3) Hille, B. *Ionic Channels of Excitable Membranes*, 2nd ed.; Sinauer, Sunderland, MA, 1992.
(4) Kolbe, M.; Besir, H.; Essen, L.-O.; Oesterhelt, D. *Science* **2000**, *288*, 1390.
(5) Weber, J. M.; Kelley, J. A.; Nielsen, S. B.; Ayotte, P.; Johnson, M. A. *Science* **2000**, *287*, 2461.
(6) Aqvist, J.; Luzhkov, V. *Nature* **2000**, *404*, 881.
(7) Williams, K. A. *Nature* **2000**, *403*, 112.
(8) Pasquarello, A.; Petri, I.; Salmon, P. S.; Parisel, O.; Car, R.; Tóth, É.; Powell, D. H.; Fischer, H. E.; Helm, L.; Merbach, A. *Science* **2001**, *291*, 856.
(9) Kielpinski, D.; Meyer, V.; Rowe, M. A.; Sackett, C. A.; Itano, W. M.; Monroe, C.; Wineland, D. J. *Science* **2001**, *291*, 1013.
(10) Kropman, M. F.; Bakker, H. J. *Science* **2001**, *291*, 2118.
(11) Robertson, W. H.; Diken, E. G.; Price, E. A.; Shin, J.-W.; Johnson, M. A. *Science* **2003**, *299*, 1367.
(12) Migliore, M.; Corongiu, G.; Clementi, E.; Lie, G. C. *J. Chem. Phys.* **1988**, *88*, 7766.
(13) Dang, L. X. *J. Chem. Phys.* **1992**, *96*, 6970.
(14) Perera, L.; Berkowitz, M. L. *J. Chem. Phys.* **1994**, *100*, 3085.
(15) Bryce, R. A.; Vincent, M. A.; Malcolm, N. O. J.; Hiller, I. H.; Burton, N. A. *J. Chem. Phys.* **1998**, *109*, 3077.
(16) Cabarcos, O. M.; Weinheimer, C. J.; Lisy, J. M.; Xantheas, S. S. *J. Chem. Phys.* **1999**, *110*, 5.
(17) Bryce, R. A.; Vincent, M. A.; Hiller, I. H. *J. Phys. Chem. A* **1999**, *103*, 4094.

(18) Vaughn, S. J.; Akhmatskaya, E. V.; Vincent, M. A.; Masters, A. J.; Hiller, I. H. *J. Chem. Phys.* **1999**, *110*, 4335.
(19) Baik, J.; Kim, J.; Majumdar, D.; Kim, K. S. *J. Chem. Phys.* **1999**, *110*, 9116.
(20) Majumdar, D.; Kim, J.; Kim, K. S. *J. Chem. Phys.* **2000**, *112*, 101.
(21) Kim, J.; Lee, H. M.; Suh, S. B.; Majumdar, D.; Kim, K. S. *J. Chem. Phys.* **2000**, *113*, 5259.
(22) Yang, X.; Wang, X.-B.; Wang, L.-S. *J. Chem. Phys.* **2001**, *115*, 2889.
(23) Lee, H. M.; Majumdar, D.; Kim, K. S. *J. Chem. Phys.* **2002**, *116*, 5509.
(24) Zhan, C.-G.; Dixon, D. A. *J. Phys. Chem. B* **2003**, *107*, 4403.
(25) Klots, C. E. *J. Phys. Chem.* **1981**, *85*, 3585.
(26) Tissandier, M. D.; Cowen, K. A.; Feng, W. Y.; Gundlach, E.; Cohen, M. H.; Earhart, A. D.; Coe, J. V. *J. Phys. Chem. A* **1998**, *102*, 7787.
(27) Tawa, G. J.; Topol, I. A.; Burt, S. K.; Caldwell, R. A.; Rashin, A. A. *J. Chem. Phys.* **1998**, *109*, 4852.
(28) Topol, I. A.; Tawa, G. J.; Burt, S. K.; Rashin, A. A. *J. Chem. Phys.* **1999**, *111*, 10998.
(29) Mejias, J. A.; Lago, S. *J. Chem. Phys.* **2000**, *113*, 7306.
(30) Friedman, H. L.; Krishnan, V. V. *Water: A Comprehensive Treatise*; Plenum: New York, 1973.
(31) Zhu, T.; Li, J.; Hawkins, G. D.; Cramer, C. J.; Truhlar, D. G. *J. Chem. Phys.* **1998**, *109*, 9117.
(32) Zhan, C.-G.; Landry, D. W.; Ornstein, R. L. *J. Am. Chem. Soc.* **2000**, *122*, 2621.
(33) Zhan, C.-G.; Dixon, D. A. *J. Phys. Chem. A* **2001**, *105*, 11534.
(34) Zhan, C.-G.; Dixon, D. A. *J. Phys. Chem. A* **2002**, *106*, 9737.
(35) Zhan, C.-G.; Bentley, J.; Chipman, D. M. *J. Chem. Phys.* **1998**, *108*, 177. Zhan, C.-G.; Chipman, D. M. *J. Chem. Phys.* **1998**, *109*, 10543. Zhan, C.-G.; Chipman, D. M. *J. Chem. Phys.* **1999**, *110*, 1611. Zhan, C.-G.; Landry, D. W.; Ornstein, R. L. *J. Phys. Chem. A* **2000**, *104*, 7672.
(36) Zhan, C.-G.; Landry, D. W. *J. Phys. Chem. A* **2001**, *105*, 1296. Zheng, F.; Zhan, C.-G.; Ornstein, R. L. *J. Chem. Soc., Perkin Trans. 2* **2001**, 2355. Zheng, F.; Zhan, C.-G.; Ornstein, R. L. *J. Phys. Chem. B* **2002**, *106*, 717. Zhan, C.-G.; Dixon, D. A.; Sabri, M. I.; Kim, M.-S.; Spencer, P. S. *J. Am. Chem. Soc.* **2002**, *124*, 2744. Dixon, D. A.; Feller, D.; Zhan, C.-G.; Francisco, S. F. *J. Phys. Chem. A* **2002**, *106*, 3191.
(37) Mallard, W. G., Linstrom, P. J., Eds. *NIST Chemistry WebBook*; NIST Standard Reference Database Number 69, February 2000; National Institute of Standards and Technology: Gaithersburg, MD, 2000 (http://webbook.nist.gov).
(38) Ruscic, B.; Feller, D.; Dixon, D. A.; Peterson, K. A.; Harding, L. B.; Asher, R. L.; Wagner, A. F. *J. Phys. Chem. A* **2001**, *105*, 1.
(39) Ruscic, B.; Wagner, A. F.; Harding, L. B.; Asher, R. L.; Feller, D.; Dixon, D. A.; Peterson, K. A.; Song, Y.; Qian, X.; Ng, C.-Y.; Liu, J.; Chen, W.; Schwenke, D. W. *J. Phys. Chem. A* **2002**, *106*, 2727.
(40) Becke, A. D. *J. Chem. Phys.* **1993**, *98*, 5648.
(41) Lee, C.; Yang, W.; Parr, R. G. *Phys. Rev. B* **1988**, *37*, 785.
(42) Stephens, P. J.; Devlin, F. J.; Chabalowski, C. F.; Frisch, M. J. *J. Phys. Chem.* **1994**, *98*, 11623.
(43) Hehre, W. J.; Radom, L.; Schleyer, P. v. R.; Pople, J. A. *Ab Initio Molecular Orbital Theory*; Wiley: New York, 1987.
(44) Dunning, T. H., Jr. *J. Chem. Phys.* **1989**, *90*, 1007.
(45) Kendall, R. A.; Dunning, T. H., Jr.; Harrison, R. J. *J. Chem. Phys.* **1992**, *96*, 6796.
(46) Peterson, K. A.; Woon, D. E.; Dunning, T. H., Jr. *J. Chem. Phys.* **1994**, *100*, 7410.
(47) Woon, D. E.; Dunning, T. H., Jr. *J. Chem. Phys.* **1995**, *103*, 4572.
(48) Purvis, G. D., III; Bartlett, R. J. *J. Chem. Phys.* **1982**, *76*, 1910.
(49) Raghavachari, K.; Trucks, G. W.; Pople, J. A.; Head-Gordon, M. *Chem. Phys. Lett.* **1989**, *157*, 479.
(50) Watts, J. D.; Gauss, J.; Bartlett, R. J. *J. Chem. Phys.* **1993**, *98*, 8718.
(51) Tomasi, J.; Persico, M. *Chem. Rev.* **1994**, *94*, 2027.
(52) Schmidt, M. W.; Baldridge, K. K.; Boatz, J. A.; Elbert, S. T.; Gordon, M. S.; Jensen, J. H.; Koseki, S.; Matsunaga, N.; Nguyen, K. A.; Su, S. J.; Windus, T. L.; Dupuis, M.; Montgomery, J. A. *J. Comput. Chem.* **1993**, *14*, 1347.
(53) Mejias, J. A.; Lago, S. *J. Chem. Phys.* **2000**, *113*, 7306.
(54) Cramer, C. J.; Truhlar, D. G. In *Solvent Effects and Chemical Reactions*; Tapia, O., Bertran, J., Eds.; Kluwer: Dordrecht, The Netherlands, 1996; p 1.
(55) Chipman, D. M. *J. Chem. Phys.* **2000**, *112*, 5558.
(56) Barone, V.; Cossi, M.; Tomasi, J. *J. Chem. Phys.* **1997**, *107*, 3210.
(57) Tomasi, J.; Mennucci, B.; Cances, E. *J. Mol. Struct. (THEOCHEM)* **1999**, *464*, 211.
(58) Cancès, E.; Mennucci, B. *J. Chem. Phys.* **2001**, *114*, 4744.
(59) Cossi, M.; Rega, N.; Scalmani, G.; Barone, V. *J. Chem. Phys.* **2001**, *114*, 5691.
(60) Chipman, D. M. *J. Chem. Phys.* **2002**, *116*, 10129.
(61) Tawa, G. J.; Topol, I. A.; Burt, S. K.; Caldwell, R. A.; Rashin, A. A. *J. Chem. Phys.* **1998**, *109*, 4852.
(62) Topol, I. A.; Tawa, G. J.; Burt, S. K.; Rashin, A. A. *J. Chem. Phys.* **1999**, *111*, 10998.
(63) Frisch, M. J.; Trucks, G. W.; Schlegel, H. B.; Scuseria, G. E.; Robb, M. A.; Cheeseman, J. R.; Zakrzewski, V. G.; Montgomery, J. A.; Stratmann, R. E.; Burant, J. C.; Dapprich, S.; Millam, J. M.; Daniels, A. D.; Kudin, K. N.; Strain, M. C.; Farkas, O.; Tomasi, J.; Barone, V.; Cossi, M.; Cammi, R.; Mennucci, B.; Pomelli, C.; Adamo, C.; Clifford, S.; Ochterski, J.; Petersson, G. A.; Ayala, P. Y.; Cui, Q.; Morokuma, K.; Malick, D. K.; Rabuck, A. D.; Raghavachari, K.; Foresman, J. B.; Cioslowski, J.; Ortiz, J. V.; Stefanov, B. B.; Liu, G.; Liashenko, A.; Piskorz, P.; Komaromi, I.; Gomperts, R.; Martin, R. L.; Fox, D. J.; Keith, T.; Al-Laham, M. A.; Peng, C. Y.; Nanayakkara, A.; Gonzalez, C.; Challacombe, M.; Gill, P. M. W.; Johnson, B.; Chen, W.; Wong, M. W.; Andres, J. L.; Gonzalez, A. C.; Head-Gordon, M.; Replogle, E. S.; Pople, J. A. *Gaussian 98*, Revision A.6; Gaussian, Inc.: Pittsburgh, PA, 1998.
(64) Anchell, J.; Apra, E.; Bernholdt, D.; Borowski, P.; Bylaska, E.; Clark, T.; Clerc, D.; Dachsel, H.; de Jong, W. A.; Deegan, M.; Dupuis, M.; Dyall, K.; Elwood, D.; Fann, G.; Fruchtl, H.; Glendenning, E.; Gutowski, M.; Harrison, R.; Hess, A.; Jaffe, J.; Johnson, B.; Ju, J.; Kendall, R.; Kobayashi, R.; Kutteh, R.; Lin, Z.; Littlefield, R.; Long, X.; Meng, B.; Nichols, J.; Nieplocha, J.; Rendall, A.; Rosing, M.;Sandrone, G; Stave, M.; Straatsma, T.;Taylor, H.; Thomas, G.; van Lenthe, J.; Windus, T; Wolinski, K.; Wong, A.; Zhang, Z. *NWChem*, Version 4.0.1; Pacific Northwest National Laboratory, Richland, WA, 2001.
(65) MOLPRO is a package of ab initio programs written by H.-J. Werner and P. J. Knowles. Werner, H. J.; Knowles, P. J.; Almlof, J.; Amos, R. D.; Berning, A.; Cooper, D. L.; Deegan, M. J. O.; Dobbyn, A. J.; Eckert, F.; Elbert, S. T.; Hampel, C.; Lindh, R.; Lloyd, A. W.; Meyer, W.; Nicklass, A.; Peterson, K. A.; Pitzer, R. M.; Stone, A. J.; Taylor, P. R.; Mura, M. E.; Pulay, P.; Schütz, M.; Stoll, H.; Thorsteinsson, T. *MOLPRO*; Universität Stüttgart and University of Birmingham: Stüttgart, Germany, and Birmingham, England, 2000.
(66) Foresman, J. B.; Frisch, A. *Exploring Chemistry with Electronic Structure Methods*, 2nd ed.; Gaussian, Inc.: Pittsburgh, PA, 1996.
(67) We estimated the entropy for structure C as follows. We replaced the two imaginary frequencies with frequencies of 23 and 29 cm^{-1} taken from our other structures. At 298 K, these two low-lying modes contribute 3.66 kcal/mol to ΔG and we corrected the overall ΔG by this amount. This makes structures B and C closer to each other but does not change the ordering of the structures when solvent effects are included.
(68) Peterson, K. A.; Xantheas, S. S.; Dixon, D. A.; Dunning, T. H., Jr. *J. Phys. Chem. A* **1998**, *102*, 2449.
(69) Feller, D.; Peterson, K. A. *J. Chem. Phys.* **1999**, *110*, 8384.
(70) Feller, D. *J. Chem. Phys.* **1992**, *96*, 6104.
(71) Feyereisen, M. W.; Feller, D.; Dixon, D. A. *J. Phys. Chem.* **1996**, *100*, 2993.
(72) Xantheas, S. *J. Chem. Phys.* **1996**, *104*, 8221.
(73) Pliego, J. R., Jr.; Riveros, J. M. *Phys. Chem. Chem. Phys.* **2002**, *4*, 1622.